ELSEVIER

Biophysical Chemistry 53 (1994) 95–104

Biophysical Chemistry

Conformational changes in yeast phosphoglycerate kinase upon substrate binding

S.J. Henderson [a,*], E.H. Serpersu [b], B.S. Gerhardt [b], G.J. Bunick [a]

[a] *Biology Division, Oak Ridge National Laboratory, Oak Ridge, TN 37831-8077, USA*

[b] *Department of Biochemistry, University of Tennessee, Knoxville, TN 37996, USA*

Received 20 August 1993; revised 10 April 1994; accepted 15 April 1994

Abstract

Small-angle neutron scattering (SANS) was used to measure the radius of gyration (R_g) of solutions of phosphoglycerate kinase (PGK) in a variety of substrate environments in D_2O. The R_g of 24.0 Å was measured for native PGK. A decrease in R_g was observed for the following: 23.7 Å for PGK + sulphate; 23.5 Å for PGK + β,γ-bidentate $Cr(H_2O)_4ATP$ (CrATP); 23.3 Å for PGK + 3-phospho-D-glycerate (PGA) + CrATP; 22.9 Å for PGK + CrATP + sulphate; 22.6 Å for PGK + PGA + CrATP + sulphate. The statistical error was about ±0.3 Å, which is less than systematic effects in this system. These results are consistent with catalysis by a hinge-bending motion of the enzyme. Since CrATP is not hydrolyzed, these results represent the conformational states of the bound substrates in the catalytically relevant ternary complex in the absence of product formation. The second virial coeffcient is also measured for this system and this is consistent with that calculated from the protein volume only.

Keywords: Yeast phosphoglycerate kinase; Small-angle neutron scattering; Second virial coefficient; Conformational change; Radius of gyration

1. Introduction

Yeast phosphoglycerate kinase (PGK) is one of several kinases for which the protein crystal structures consist of two domains separated by the substrate binding cleft (Fig. 1). The locations of the proposed binding sites for substrates and the bilobal structure of the enzyme led to the suggestion that closing of the active site occurs via a hinge-bending action [1–3]. The substrates for PGK are adenosine triphosphate (ATP) and 3-phospho-D-glycerate (PGA). Substrate-induced conformational changes in yeast PGK have been observed by various techniques, including NMR [4–6], small-angle X-ray scattering (SAXS) [3,7,8], analytical ultracentrifugation [9], and site specific mutations [10–13]. SAXS studies of yeast [3] and pig muscle enzyme [14] indicated a decrease in the radius of gyration (R_g) for these enzymes in the presence of substrates. Although there is no direct crystallographic evidence, these results are consistent with hinge-bending motion upon formation of the ternary complex. Indeed, the X-ray structure of the binary pig muscle enzyme–PGA complex shows that the domains are closer to each other when compared to the substrate-free horse muscle enzyme [15], although not to the extent suggested for the ternary complex. Simple hinge-bending motion (rotation of two lobes about a single axis) of the two domains is not compatible, however, with the determined substrate-to-enzyme distances in binary CrATP–PGK and ternary CrATP–

* Corresponding author.

SSDI 0301-4622(94)00080-4

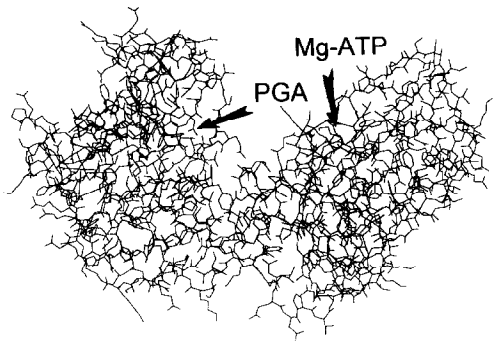

Fig. 1. Two-dimensional representation of the PGK crystal structure from the Brookhaven data bank.

PGA–PGK complexes [16], which suggests a more complex rearrangement.

The structural interpretation of the solution studies has not been straightforward with yeast PGK since the only known crystal structure of the yeast enzyme is solved in the presence of effector sulfate ion. Sulfate and other multivalent anions such as inorganic phosphate are known to affect the kinetics and the interaction of the enzyme with substrates [17,18]. At low concentrations, sulfate activates the enzyme and at high concentrations, it is a competitive inhibitor [17,18]. NMR [5,19–21], hydrodynamic [9], and other binding [17,22] studies also suggest that the presence of sulfate ion alters substrate binding and the structure of the enzyme–substrate complexes as well as the equilibrium of the bound substrates. Site specific mutations of different residues yielded various mutant enzymes, some of which lack activation by sulfate [11,12,23–25]. However, the nature and the extent of the conformational change induced by sulfate is not known. A recent NMR study of internuclear distances reported the arrangement of the substrates at the active site which are significantly altered by the presence of sulfate ion [23].

The results of an earlier hydrodynamic study suggested that PGK becomes 'more compact' in the presence of both substrates [9]. Furthermore, the authors also reported that the same effect was produced by the presence of sulfate ion in the absence of substrates. Although values for binary enzyme–substrate complexes were reported, no information was given on the ternary, catalytically relevant, complex in the presence of sulfate. The validity of these results, however, has been questioned [7] and conflicting ultracentrifugation studies indicating no difference in $s_{20,w}$ values of the enzyme in the absence and presence of the substrates with and without sulfate has been reported [26]. The latter investigators, however, exclude the catalytically required divalent metal ion which affects the binding of substrates to the enzyme [19].

This report describes an investigation of the low resolution structure of native PGK and 'closed' conformations with the substrates and/or sulfate ion by small-angle neutron scattering (SANS). A preliminary report of this work was previously presented [27]. Previous SAXS studies were performed in the presence of high concentrations of substrates with the enzyme at 25°C [3,9], which were therefore done with an equilibrium mixture of the substrates and products which also yields inorganic phosphate upon hydrolysis of 1,3-bis-PGA. Furthermore, the change due to sulfate ion was not investigated in those studies. In this study, we used an exchange-inert MgATP analog, namely β,γ-bidentate $Cr(H_2O)_4ATP$ (CrATP), and we investigated not only the conformational effects of substrates, but sulfate as well. CrATP is a competitive inhibitor of the enzyme [28,29] and slowly inactivates PGK by forming a stable complex with a 1:1 stoichiometry in the presence of PGA and/or sulfate ion [30]. Since CrATP is not hydrolyzed by the enzyme [31], no product formation was possible in our experimental conditions. In the previous SAXS studies, the authors used high concentrations of MgATP and PGA. Under their experimental conditions, the reaction product 1,3-*bis*-PGA quickly hydrolyzes to yield PGA and inorganic phosphate ($t_{1/2} \approx 20$ min). Since phosphate affects the enzyme just like sulphate, earlier results represent the effects of not only bound substrates but bound products and effector anions as well. Thus, multiple conformations of the enzymes could be present.

2. Experimental procedures

2.1. Materials

PGK was isolated from yeast strain 20B-12 containing multi-copy plasmid pCGY219. The plasmid and the yeast strain were kindly provided by Dr. Hitzeman of Genentech Inc. The purification of the enzyme was accomplished as described earlier [32,33]. The enzyme was greater than 95% pure as determined by

SDS-PAGE. A specific activity of ≈580 μmol/min mg was observed for the purified enzyme when assayed under saturating substrate concentrations (3 mM for both CrATP and 3PGA) in the absence of sulfate at 25°C, pH 7.5. The enzyme concentration was determined at 280 nm using $\varepsilon_{1\,cm}^{0.1\%} = 0.5$. The CrATP was prepared [34] immediately before use, diluted with D_2O and used in the inactivation experiments. D_2O (99.9 d%) was purchased from Isotec and Cambridge Isotope Laboratories. All other chemicals used were of the highest grade commercially available. Stock solutions of buffer, salts and substrates were prepared in D_2O. The pH of solutions in D_2O is reported as read directly from the pH meter, and is designated pH*.

2.2. *Enzyme preparation*

The enzyme (30–40 mg/ml) was incubated for 120 min at 37°C in a total volume of 1.7 ml D_2O containing 50 mM MES pH* 5.9, 100 mM NaCl and 3 mM CrATP. This pH* was selected because of the instability of CrATP complex at higher values [34]. Previous studies indicated that the kinetics of the enzyme is not altered at this pH* [24]. When present, the concentrations of PGA and/or sulfate ion were 3 and 10 mM, respectively. When sulfate ion was present, the ionic strengths of the solutions were adjusted by lowering the NaCl concentration. The activity of the enzyme was determined spectrophotometrically at 340 nm, by measuring the initial rates in a coupled enzyme assay as described earlier [30,35] in a total volume of 1 ml at 25°C. The solutions containing the inactivated enzyme (15% remaining activity) were then centrifuged 10 min at 10000 g to remove aggregated protein. These solutions were stored on ice until use.

The inactivation of yeast PGK with CrATP was carried out in two groups. In each group, the three incubation conditions were:

(a) native PGK;

(b) PGK in the presence of CrATP and;

(c) PGK in the presence of CrATP and PGA.

The first group contained 100 mM NaCl and the second group contained 10 mM Na_2SO_4 and an appropriate concentration of NaCl to match the ionic strength in both groups. In all experiments, the conditions were chosen such that PGA and CrATP were saturating (3 mM at highest PGK concentration) and the residual activity of the enzyme was less than 15% at the end of incubation period. SANS experiments were then performed with the above solutions as a function of enzyme concentration. At the end of neutron scattering experiments, no loss of enzymatic activity from the native PGK was detected.

2.3. *Small-angle neutron scattering (SANS) measurements.*

The experiments were conducted at the W.C. Koehler 30 m SANS camera at Oak Ridge National Laboratory. The neutron wavelength (λ) was 4.75 Å ($\Delta\lambda/\lambda \approx 5\%$) and the beam diameter at the sample was 16 mm. The sample detector distance was 3.63 m, which gave the first usable data at $q \approx 0.022\,Å^{-1}$, where q is the momentum transfer for the scattering event defined as

$$q = 4\pi\lambda^{-1} \sin\theta \qquad (1)$$

and 2θ is the scattering angle. The samples were contained in cylindrical quartz cells of path length 5.00 mm. The area detector was 64 cm × 64 cm with a pixel area of 1 cm^2. The data were reduced with the program SPECTOR (author John Hayter) on a pixel by pixel basis for detector efficiency, instrumental background and solvent (buffer) background prior to azimuthal averaging to produce one-dimensional data. The net intensities were converted to an absolute (±5%) differential cross-section per unit sample volume ($d\Sigma/d\Omega(q)$ in units of cm^{-1}) by comparison with precalibrated secondary standards [36]. The detector efficiency calibration was based on the scattering from light water. Data were recorded at about 7°C.

3. Results and discussion

SANS experiments were performed in D_2O solutions since the replacement of H_2O with D_2O improves the signal-to-noise ratio significantly due to lower incoherent scattering of D_2O. There is also a greater neutron scattering density difference or contrast (Eq. (2), see below) between the normally hydrogenated enzyme and D_2O solution (typically $\Delta\rho = -3.5 \times 10^{10}\ cm^{-2}$ for H-proteins with 80% of labile hydrogens exchanged) compared to an H_2O solution (typically $\Delta\rho = +2.35 \times 10^{10}\ cm^{-2}$ for H-proteins), where contrast is defined as

$$\Delta\rho = \rho_{\text{solute}} - \rho_{\text{solvent}} \quad (2)$$

and

$$\rho = \Sigma\, b_i / V\,,$$

where the b_i are the neutron scattering lengths of all the atoms contained in the solvent excluded volume V. The scattered intensity from an isolated protein molecule at zero angle is related to contrast as

$$I(q)|_{q=0} = (\Delta\rho)^2 V^2\,, \quad (3)$$

where $I(q)$ is used instead of the differential cross-section nomenclature for simplicity.

The observed intensity in an experiment on a monodisperse sample can be written as the differential scattering cross-section per unit solid angle per unit volume,

$$\mathrm{d}\Sigma/\mathrm{d}\Omega(q) = I(q) = nP(q)S(q)\,, \quad (4)$$

where $P(q)$ is called the particle form factor (different for X-rays compared to neutrons) and describes the scattering from an isolated particle, $S(q)$ is called the interparticle structure factor which is an interparticle term that converges to unity at infinite dilution independent of the radiation used, and n is the number density of the particles (number/cm^3).

Ligand-induced conformational changes would be detected with greater precision in D_2O due to this higher intensity and the much lower incoherent scattering from deuterium compared to hydrogen (incoherent scattering superposes a flat signal onto the data, which is greater than the actual signal in the case of H_2O solvent). The kinetics of yeast phosphoglycerate kinase is not altered by the presence of D_2O as solvent with the exception of a lower $V_{\max}$ [42].

When the radius of gyration is sought for the isolated particle, a concentration series is usually done and the R_g measurements are extrapolated linearly to $c=0$ as $(R_g)^2$ against c. The radius of gyration of a particle is the mean square radius of all volume elements from the center of mass, where these elements are weighted by their contrast value. It is possible to have a large conformation change with no change in R_g, such as when one lobe of a bi-lobal protein rotates, without altering the lobe–lobe seperation or lobe shape. R_g is calculated in these experiments from the Guinier formula which models the low q portion of the scattering curve (typically quoted as $qR_g < 1$, though this q domain is a strong function of the protein shape) by

$$P(q) = P(0)\,\exp(-\tfrac{1}{3}[\,qR_g]^2)\,. \quad (5)$$

For all real measurements on particles in solution, the qR_g domain chosen will give an estimate of R_g at infinite dilution either higher or lower than the true R_g that would be measured if the qR_g domain measured were infinitesimally small (say, $qR_g < 0.05$). This deviation is usually ignored in small-angle scattering work. It can be estimated for any particular study such as PGK by studying the Guinier estimate of R_g as a function of q domain for the scattering either from the crystal coordinates or from some other model. The upper limit of qR_g for Eq. (5) can vary by more than an order of magnitude (less than $0.2 < [qR_g]_{\max} <$ more than 2.0) if a 1% deviation in the R_g estimate from [5] away from the true R_g is used as a criterion (arbitrary) for validity. This value of $[qR_g]_{\max}$ is, of course, a function of the lowest qR_g at which data is measured, where $[qR_g]_{\max}$ is reduced as $[qR_g]_{\min}$ increases.

Consider two identical, uniform ellipsoids ($a=b=16$ Å, $c=24$ Å), with ellipsoid A at the origin and ellipsoid B parallel to A at (32, 0, 0), i.e. touching, with R_g(true) = 21.76 Å. This model (conformation No. 1) of a bilobal structure has valid qR_g domains 0.17–2.3, and/or 1.0–2.1, and so on. So even data entirely outside the 'classical' Guinier domain ($qR_g < 1$) can give a good R_g estimate for this model. Conformation No. 2 is created from the first when ellipsoid B is rotated 90° about the x axis, and so the true R_g is unchanged, and the valid qR_g domains are unchanged from conformation No. 1, even though the scattering curve has changed. Conformation No. 3 is created from the first when ellipsoid B moves another 3 Å away from ellipsoid A to (35, 0, 0), and each ellipsoid rotates about their own b axes 20° (and −20°), tilting together to touch (forming a 'V' with 40° between the two c axes). The true R_g is now 22.89 Å, and the values of $[qR_g]$max for the above valid domains are lowered to 1.9 and 1.65 (from 2.3 and 2.1, respectively). This reduction is produced by moving the ellipsoid centers apart and is independent of tilt. The crystal coordinates of PGK are known (3PGK, Brookhaven Protein Data Bank), so these can be used to generate the scattering curve from the crystal as if it were placed in water. Crystalline PGK has a valid Guinier domain (the 1% criterion used above) of $0.14 < qR_g < 1.84$, which is

Table 1
R_g summary for different substrate conditions

System	c (mg/ml)	R_g (Å)	$(I_0/c)_{c=0}$ (cm²/g)
crystalline PGK	–	24.1	46.1
native PGK	5, 10, 20, 30	24.0 ± 0.2	46.4
PGK + SO_4	10, 20, 30	23.7 ± 0.4	36.9
PGK + CrATP	8.2, 18, 27	23.5 ± 0.3	42.0
PGK + CrATP + PGA	4.5, 7.4, 18, 27	23.3 ± 0.2	41.3
PGK + CrATP + SO_4	(4.4), 18, 26	22.9 ± 0.4(?)	34.9
PGK + CrATP + PGA + SO_4	4.5, 8.4, 18, 27	22.6 ± 0.2	36.2

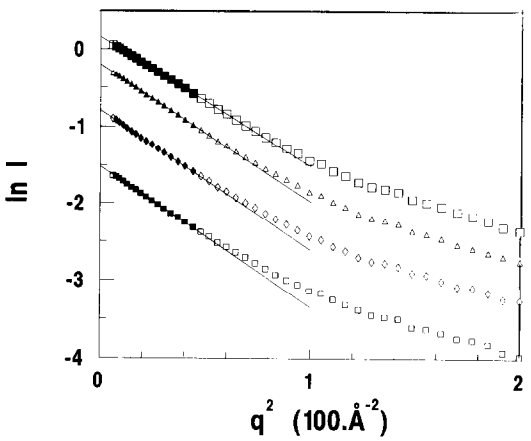

Fig. 2. Guinier plot of ln I against q^2 for native PGK at four concentrations: 5, 10, 20, 30 mg/ml, showing the points used (filled symbols) to measure R_g.

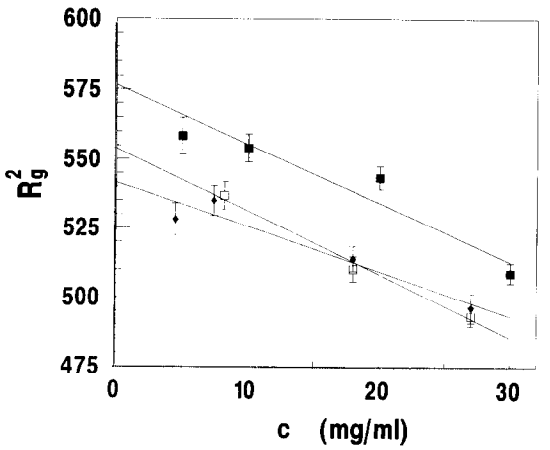

Fig. 3. Plot of R_g^2 against c for the 3 sulphate-free cases: (■) native PGK; (□) PGK + CrATP; (♦) PGK + PGA + CrATP.

similar to the above model system. From this simple illustration, we assert that for contracting bi-lobal proteins of similar proportions (such as PGK), the valid Guinier range observed from the crystal structure, if known, is valid for the contracted (i.e. substrates bound) forms, where the contractions are small ($\leq 5\%$). In addition, we use a different qR_g domain for the PGK + sulphate case (due to suspected slight aggregation), and we use the crystal scattering curve to estimate the correction term to correctly compare the two domains. The qR_g domain 0.9–1.8 was used for our data for the PGK + sulphate case and the domain 0.6–1.5 was used for all others. The corrections that would be required for the crystal scattering in these two q ranges to give the true crystal R_g are +0.15 and +0.34 Å respectively, which are applied to our data. The small size of these corrections along with the above arguement makes them useful and valid in our case to improve the precision of the data. We do not claim that all systems are amenable to such treatment.

For the case of PGK + CrATP + sulphate, the R_g for the lowest concentration is significantly displaced from the trend shown in the other experiments, so the slope drawn in Fig. 4 is taken from the two highest concentrations only and a larger error is assigned to the infinite dilution result. The data correction for deconvolution of wavelength spread (5%) and neutron beam size was estimated from Ref. [37]. The correction was negligible (about +0.02 Å increase in R_g) so was ignored (Table 1, Figs. 2–4).

The data were also corrected for excess incoherent scattering from the protein compared to the buffer. The incoherent correction produced a difference in R_g of, for example, +0.13 Å for 5 mg/ml native PGK. This

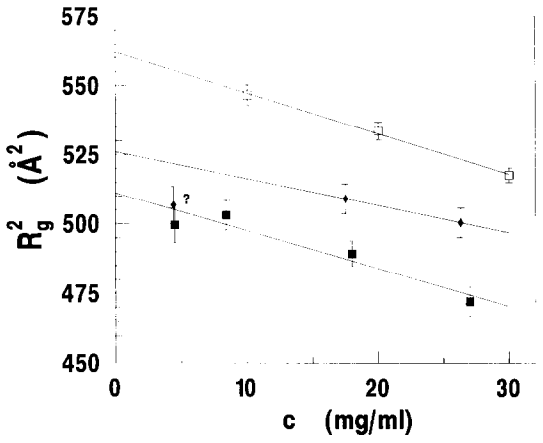

Fig. 4. Plot of R_g^2 against c for the 3 sulphate-containing cases: (□) PGK + sulphate; (◆) PGK + CrATP + sulphate; (■) PGK + PGA + CrATP + sulphate.

correction was made as follows. The scattering intensity from the buffer was measured at 0.068 cm^{-1}, of which 50% is assumed to be incoherent scattering [38]. The incoherent scattering of the sample is assumed proportional to the fraction of the beam not transmitted by the sample, $1-T$, where T is the transmission of the cell contents. Then,

$$I_{sample}(inc) = 0.034[(1-T_{sample}/0.95) / (1-T_{buffer}/0.95)], \quad (6)$$

where 0.95 is the transmission of the empty cell. This agreed within 50% of the value calculated directly by multiplying the number of hydrogen atoms per cm^3 by the incoherent cross-section of hydrogen 80 b), and dividing by 4π.

The 5.0 mm path length is longer than the more traditional length of 2.0 mm for D_2O solutions. The 20 mg/ml native PGK sample was measured with both 2.0 and 5.0 mm path lengths to give R_g of 23.21 ± 0.07 Å (2.0 mm) and 23.32 ± 0.09 Å (5.0 mm), as well as $I(0)$ values which agree within the accuracy of the transmission measurements.

SAXS studies have been reported on yeast PGK [3,7,8]. These are tabulated in Table 2 for comparison to this work. The other experiments were X-ray experiments which should produce somewhat higher R_g due to the following factors:

(a) X-rays are scattered by electron density differences between the protein and the solvent, while the neutrons are scattered by nuclear scattering length density differences between the same. These are not equivalent. The atomic coordinates of the crystal can be used to estimate the R_g for each case. We assume that 80% of the labile hydrogen atoms exchange with the solvent in random positions (in reality, an unknown fraction would actually exchange in specific, solvent accessible positions, which is difficult to predict from the crystal coordinates), and we assume a specific volume of 0.72 cm^3/g. We calculate R_g(crystal/neutron) = 24.13 Å and R_g(crystal/X-ray) = 24.30 Å so the difference is −0.17 Å for the neutron case.

(b) The measurement of hydration is probably more significant when comparing the X-ray and neutron scattering because, although the protein is hydrated in both cases, the opposite sign of the contrast of protein against the solvent makes the solvent perturbation to the R_g opposite also. If we model a 3 Å thick layer of water on the protein with a 5% greater density compared to bulk water (arbitrary choice), we see a ΔR_g of +0.47

Table 2
Comparison of R_g (Å) determinations with other work

System	Ref. [7]	Ref. [8]	Ref. [3]	This work
temperature (°C)	20	not given	25	7
pH	7	7	not given	5.9
q for R_g estimate	–	–	0.013–0.067	0.025–0.064
PGK native	24.5	24.5 ± 0.2	23.3 ± 0.2	24.0 ± 0.2
PGK + PGA + MgATP	23.3	23.2 ± 0.2	22.3 ± 0.3	22.6 ± 0.2[a]
PGK + PGA	–	–	23.0 ± 0.2	–
PGK + MgATP	23.8	–	22.8 ± 0.2	23.5 ± 0.3[a]

[a] CrATP was used instead of MgATP in this work

Å for X-rays and −0.34 Å for neutrons relative to the unhydrated cases, or a net −0.81 Å from hydration for the neutron case.

Therefore, this modelled hydration case ((a) and (b)) gives a total ΔR_g of −1.0 Å for the neutron relative to the X-ray case.

The R_g of a protein can be sensitive to both conformation changes and/or hydration changes. A conformation change, however, should produce no change in $(I_0/c)_{c=0}$ because the volume and contrast are unchanged. A hydration change can produce a change in $(I_0/c)_{c=0}$, since the effective scattering object is changing in size and composition. R_g measurements are more sensitive to hydration effects when $|(\rho_{solvent}/\Delta\rho)|$ is relatively large. For our system of H-protein in D_2O, we define an increase in hydration to mean an increase in the average density of water at the surface of the protein due to higher surface charge there (which disrupts the relatively open structure of bulk water). (This would also be associated with associating/dissociating of ions/substrates which are ignored in the following calculation on the effect of changing the density of a uniform layer of water around the protein.) This hydration increase will lower the R_g, even though the scattering object is physically larger, because the hydration layer is a positive contrast perturbation on the dominant negative contrast of the protein. Similarly, $(I_0/c)_{c=0}$ will also decline. From Refs. [3,4], we calculate $(I_0/c)_{c=0}$ as 46.1 cm^2/g (using $\Delta\rho = -3.45 \times 10^{10}\ cm^{-2}$, protein specific volume = 0.72 cm^3/g, M_w = 44.6 kDa). From Table 2, we see that native PGK agrees well with this, and the PGK + CrATP/PGK + CrATP + PGA cases are 10% lower at about 42, but the three systems containing sulphate are about 20% lower at about 36. Hydration changes would manifest as discrete effects at surface sites rather than a uniform global change over the whole surface. We do not know the detailed information required to model real hydration with PGK. However, it is useful to look at uniform global hydration on PGK and its relative effect on $(I_0/c)_{c=0}$ and R_g, in order to try to distinguish between changes in conformation and hydration. For a 3 Å hydration thickness of D_2O, with 5% higher density than the bulk, the R_g is reduced by 0.3 Å and the $(I_0/c)_{c=0}$ is reduced by 10%. For a 10% higher density in the hydration layer, the R_g is reduced by 0.7 Å and the $(I_0/c)_{c=0}$ is reduced by 19%. These calculations imply large hydration effects are occurring, particularly when sulphate is present. Application of these calculations to the figures in Table 1 suggest that for the systems PGK + CrATP, PGK + CrATP + PGA, and PGK + SO_4, the observed R_g changes are consistent with hydration alone. The systems PGK + CrATP + SO_4 and PGK + CrATP + PGA + SO_4 have conformation changes convoluted with hydration changes. The earlier small-angle X-ray scattering studies did not discuss the conflicting effects of hydration in their conformation studies. For X-rays, greater hydration will increase R_g and $(I_0/c)_{c=0}$, though no evidence of this is apparent from Table 1, which shows similar differences to this neutron study, rather than larger differences. This may be due to solution conditions being different than those used here, including the use of MgATP, giving rise to an equilibrium mixture of substrates and products. This could be checked by repeating our experiment with SAXS. While comparison of absolute R_g between publications is complex because of reasons outlined above, R_g differences within publications are more clearly defined and hence comparable.

The effects of multivalent anions such as sulfate or phosphate on the structure and the activity of PGK has been studied [5,9,17–22]. It was also shown recently that the presence of sulphate not only alters the enzyme conformation and activity but also changes the conformation and arrangement of the substrates at the active site as determined by NMR studies [24]. Roustan et al. reported [9] that PGK becomes more 'compact' when both substrates are present. The same effect was produced by the presence of sulphate even in the absence of substrates as determined by hydrodynamic studies [9]. These studies, however, did not report the effects of sulphate on the catalytically relevant PGK + MgATP + PGA complex. Recent sedimentation studies yielded conflicting results suggesting that the hydrodynamic properties of PGK are not altered by the presence of substrates and sulfate [26], though these authors excluded the catalytically required Mg^{2+} to prevent catalysis. The results of Roustan et al. [9] were also regarded as 'rather strange' by Ptitsyn et al. [7] because it would indicate significant changes in the molecular dimensions of PGK.

Proteins do not form ideal solutions because the spatial dispositions of the particles are not independent. The scattered intensity of neutrons (or X-rays) is not just the summation of the scattering from individual protein molecules. McMillan and Mayer [39] rigor-

Table 3
Variation in PGK contrast (calculated) as a function of H–D exchange with the solvent D_2O

H–D exchange at labile sites (D%)	Contrast (10^{10} cm^{-2})
0	−4.57
80	−3.50
100	−3.23

ously derived a series expansion for osmotic pressure in terms of concentration, which is written as

$$p = RT(c/M_w + A_2c^2 + A_3c^3 + \ldots) , \quad (7)$$

where M_w is the molecular weight of the solute, and c is the concentration of the solute in g/cm^3, and the A_n are called the virial coefficients which are constant at constant temperature. This series converges and is valid at any concentration. The coefficients A_n are related to the molecular distribution functions, in particular, A_2 has a fairly simple molecular meaning describing pairwise particle–particle interactions. The third term (A_3) involves interactions between triplets of molecules and so on. The second virial term accounts quantitatively for deviations from ideality quite well for many cases where c is not too high.

If the solute particles repel one another with a force which falls off rapidly with distance, the second virial coefficient can be described [40] in the form

$$A_2 = (N_A/M_w^2)(b + a/RT) , \quad (8)$$

where N_A is Avogadro's number, b is the covolume (cm^3) or effective volume and a is a constant with a positive sign proportional to the energy of repulsion. Repulsion between the particles increases the effective volume of the particle. For proteins, the magnitude of a would be minimal at the isoelectric point and/or in high salt conditions. For cases well away from the isoelectric point and low salt, higher terms in the virial series are needed to correctly interpret scattering and other measurements. For a spherical particle, the covolume is equal to four times the actual volume, which is equal to the volume excluded from the center of an approaching second identical sphere. Few measurements of A_2 for protein solutions appear to have been made [16], and none from SAXS or SANS to our knowledge.

From Eqs. (3) and (4), we can write

$$M_{w-app} = [\ 1000\, N_A I(0)\ ] / [\ cv^2(\Delta\rho)^2\ ] , \quad (9)$$

where v is the specific volume of protein (typically ≈ 0.72 cm^3/g) and $M_{w\text{-app}}$ is the apparent molecular weight. From Ref. [41], we see how the true molecular weight derives from the apparent molecular weight and the second virial coefficient,

$$M_{w-app} = M_w / [\ 1 + 2A_2cM_w\ ] , \quad (10)$$

and combining Eqs. (9) and (10, we get

$$c/I(0) = K[\ 1 + 2A_2cM_w\ ] , \quad (11)$$

where

$$K = N_A / [\ M_w v^2 (\Delta\rho)^2\ ] \quad (12)$$

so a plot of $c/I(0)$ against c will be linear (assuming two terms in the virial series describes the system) to give A_2 from the slope and K from the intercept. The theoretical value of $\Delta\rho$ is a strong function of the amount of H/D exchange exhibited as shown by Table 3, which contributes perhaps $\pm 15\%$ error to K(calc.). There is also $\pm 5\%$ uncertainty from v^2, so

K(calc.) $= 21.9 \pm 4.3$ mg/cm^2.

This number agrees with the measured values for K for the three non-sulphate cases (Table 4, Fig. 5). All solutions had the same ionic strength. The calculated

Table 4
Summary of A_2 values for different substrate conditions

System	c (mg/ml)	A_2M_w (cm^3/g)	K (mg/cm^2)
PGK + PGA + CrATP	4.5, 7.4, 18, 27	3.15	24.2
PGK + CrATP	8.2, 18, 27	3.02	23.8
PGK + SO_4	10, 20, 30	1.56	27.1
PGK + CrATP + SO_4	(4.4), 18, 26	6.29	28.7
PGK + PGA + CrATP + SO_4	4.5, 8.4, 18, 27	5.64	27.6

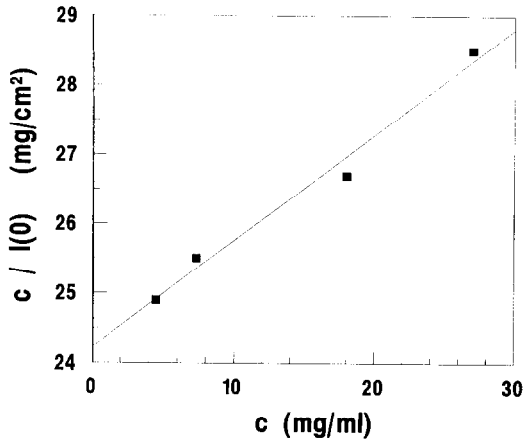

Fig. 5. Virial coefficient plot for PGK + PGA + CrATP.

concentration slope in Eq. (11) (using Eq. (8) with $a=0$) is 0.127 cm, or $A_2M_w=2.9$ cm^3/g ($M_w=44.6$ kDa) which is also close to that observed for the three non-sulphate cases.

The three sulphate-containing cases are systematically different in intercept and slope. Because the ionic strength was kept the same as with the non-sulphate cases, there is less charge shielding the protein molecules, so data at lower concentrations may be required to correctly measure A_2 (due to higher virial terms being involved). The higher slope may be from lower screening (more repulsion) between the molecules (so A_2 is larger). The higher intercept reflects the strong hydration discussed earlier. The low slope for PGK + sulphate indicates an attractive potential (Eq. (8)) with low screening which is supported by the presence of slight aggregation observed with this sample.

4. Conclusion

The results of SANS experiments presented here show that the radius of gyration of PGK is reduced by 0.7 Å when the substrates are bound to the enzyme (Table 1) without sulphate compared to 1.4 Å with sulphate. Similar observations were made earlier in SAXS experiments where binding of substrates to yeast and muscle enzymes produced R_g changes of ≈ 1.2 Å between the free enzyme and the ternary enzyme–MgATP–PGA complex [3,7]. An important difference between our conditions and the X-ray scattering conditions is our prevention of unwanted product formation. We used exchange–inert CrATP as the metal–ATP analog, that binds to the active site and inactivates the enzyme in the presence and absence of PGA [30]. Thus, the binary PGK + CrATP and ternary PGK + PGA + CrATP complexes contain the locked conformation of PGK. An examination of the earlier data reveals that under the conditions for SAXS [3,7], substrates and products were in equilibrium. Furthermore, since the product 1,3-bis-PGA is unstable in solution and hydrolyzes to 3-PGA and phosphate, the observed change of -1.2 Å in R_g for SAXS may reflect the combined effects of bound substrates and products; multivalent anions such as phosphate also affects PGK just like sulphate. The determined ΔR_g values of SAXS and SANS experiments are not consistent when allowing for hydration effects, but when all substrates are present including sulphate, cleft closure between the two protein domains is supported [1–3].

Other authors [3,7] did not investigate the effects of sulphate with SAXS. The presence of sulphate resulted in a larger change in the radius of gyration upon formation of the ternary complex, due in part to unusually large hydration effects. These observations suggest that multivalent anions have distinct and independent effects on the the enzyme, which are revealed in this work and warrant further study. It is also clear that sulfate binds to the ternary complex suggesting the presence of anion binding sites on the enzyme distinct from the active site.

Acknowledgements

This research has been sponsored by the Office of Health and Enviromental Research, USDOE, under contract No. DE-AC05-84OR21400 with Martin Marietta Energy Systems, Inc., and NIH Grant Nos. GM29818 and GM42661.

References

[1] R.D. Banks, C.C.F. Blake, P.R. Evans, R. Haser, D. Rice, G.W. Hardy, M. Merreit and A.W. Phillips, Nature 279 (1979) 773.
[2] C.C.F. Blake and D.W. Rice, Phil. Trans. Roy. Soc. London A 293 (1981) 93.
[3] C.A. Pickover, D.B. McKay, D.M. Engelman and T.A. Steitz, J. Biol. Chem. 254 (1979) 11323.

[4] P. Tanswell, E.W. Westhead and R.J.P. Williams, Eur. J. Biochem. 63 (1976) 249.
[5] M.R. Wilson, R.J.P. Williams, J.A. Littlechild and H.C. Watson, Eur. J. Biochem. 170 (1988) 529.
[6] H.C. Graham and R.J.P. Williams, Eur. J. Biochem. 197 (1991) 81.
[7] O.B. Ptitsyn, M.Y. Pavlov, M.A. Sinev and A.A. Timchenko, in: Multidomain proteins, eds. L. Patthy and P. Friedrich (Akadémiai Kiadó, Budapest, 1986) pp. 9–25, .
[8] A.A. Timchenko and S.N. Tsyuryupa, Biophysics 27 (1982) 1065.
[9] C. Roustan, A. Fattoum, R. Jeanneau and L.A. Pradell, Biochemistry 19 (1980) 5168.
[10] M.A. Sherman, S.A. Dean, A.M. Mathiowetz and M.T. Mas, Protein Eng. 4 (1991) 935.
[11] H.C. Joao, N. Taddei and R.J.P. Williams, Eur. J. Biochem. 205 (1992) 93.
[12] M. Desmadril, P. Minard, N. Ballery, S. Gaillard-Miran, L. Hall and J.M. Yon, Proteins 10 (1991) 314.
[13] W.J. Fairbrother, P.A. Walker, P. Minard, J.A. Littlechild, H.C. Watson and R.J.P. Williams, Eur. J. Biochem. 183 (1989) 57.
[14] M.A. Sinev, O.I. Razgulyaev, M. Vas, A.A. Timchenko and O.B. Ptitsyn, Eur. J. Biochem. 180 (1989) 61.
[15] K. Harlos, M. Vas and C.F. Blake, Proteins 12 (1992) 133.
[16] K.M. Pappu and E.H. Serpersu, J. Magn. Reson., in press.
[17] R.K. Scopes, Eur. J. Biochem. 91 (1978) 119.
[18] M.M. Khamis and M. Larsson-Raznikiewicz, Biochim. Biophys. Acta 657 (1981) 190.
[19] B.D.N. Rao, M. Cohn and R.K. Scopes, J. Biol. Chem. 253 (1978) 8056.
[20] B.D. Ray and B.D.N. Rao, Biochemistry 27 (1988) 5579.
[21] W.J. Fairbrother, H.C. Graham and R.J.P. Williams, Eur. J. Biochem. 190 (1990) 161.
[22] J.A. Wrobel and R.A. Stinson, Eur. J. Biochem. 85 (1978) 345.
[23] M.T. Mas, J.M. Bailey and Z.E. Resplandor, Biochemistry 27 (1988) 1168.
[24] J.D. Gregory and E.H. Serpersu, J. Biol. Chem. 268 (1993) 3880.
[25] M.T. Mas, Z.E. Resplandor and A.D. Riggs, Biochemistry 26 (1987) 5369.
[26] M.T. Mas and Z.E. Resplandor, Proteins 4 (1988) 56.
[27] E.H. Serpersu, S.J. Henderson and G.J. Bunick, FASEB (1993) J. 7, A1175 (Abstract) and American Crystallographic Meeting, Albuquerque, NM, May 1993 Abstract PR23
[28] P.A. Walker, J.A. Littlechild, L. Hall and H.C. Watson, Eur. J. Biochem. 183 (1989) 49.
[29] D. Dunaway-Mariano and W.W. Cleland, Biochemistry 19 (1980) 1506.
[30] E.H. Serpersu, L. Summitt and J.D. Gregory, J. Inorg. Biochem. 48 (1992) 203.
[31] A.K. Jaffe, J. Nick and M. Cohn, J. Biol. Chem. 257 (1982) 7650.
[32] R.K. Scopes, Biochem. J. 122 (1971) 89.
[33] K.D. Kulbe and M. Bojanovski, Methods Enzymol. 90 (1982) 115.
[34] D. Dunaway-Mariano and W.W. Cleland, Biochemistry 19 (1980) 1496.
[35] T. Bucher, Naturwissenschaften 30 (1942) 756.
[36] G.D. Wignall and F.S. Bates, J. Appl. Cryst. 20 (1986) 28.
[37] D.I. Svergun, A.V. Semenyuk and L.A. Feigin, Acta Cryst. A44 (1988) 244.
[38] R.P. May, K. Ibel and J. Haas, J. Appl. Cryst. 15 (1982) 15.
[39] W.G. McMillan and J.E. Mayer, J. Chem. Phys. 13 (1945) 276.
[40] G. Oster, J. Gen. Physiol. 33 (1950) 445.
[41] P. Lindner and T. Zemb, eds., Neutron, X-ray and light scattering as an investigate tool for colloidal and polymeric systems (North-Holland, Amsterdam, 1991) p. 26.
[42] E.H. Serpersu, unpublished data.